

ACTIVE GALACTIC NUCLEI AND GALAXY FORMATION

ARATI CHOKSHI

Indian Institute of Astrophysics, Bangalore, India
Received 1996 November 25; accepted 1997 June 9

ABSTRACT

It is proposed that early jet-induced activity around active galactic nuclei (AGNs) is responsible for triggering large-scale star formation in protogalaxies and results in the formation of giant ellipticals and spheroids in the universe. Specifically, Begelman & Cioffi's model for overpressured cocoons expanding into protogalactic environs yields size estimates that roughly correspond to those observed in present-day ellipticals. Within this framework, the most energetic radio jets trigger the formation of large ellipticals, while the systems with lower jet energies are responsible for the formation of smaller spheroids and bulges of galaxies. Further, the evolution of AGNs with redshift also explains the observed local density of spheroids.

Such a scenario naturally accommodates a wide variety of astrophysical observations, including the origin of the infrared Hubble diagram for the most powerful radio galaxies, the origin of galaxy morphologies, the existence of a morphology-density relation in galaxy clusters, angular correlations of QSOs, the observed properties of the highest redshift galaxies, and the correlation of central black hole mass with bulge luminosity in nearby galaxies.

Subject headings: galaxies: active — galaxies: elliptical and lenticular, cD — galaxies: formation — galaxies: jets

1. INTRODUCTION

Since the earliest models of protogalaxies by Partridge & Peebles (1967), searches for forming galaxies have been designed to identify that early epoch when most of the gas in a galaxy is converted into stars in a starburst phenomenon that takes place on timescales that are short compared to the evolutionary timescales of galaxies. In the present paper, we use “galaxy formation” as corresponding to the primary episode of large-scale star formation in gaseous protogalactic environments that converts a large fraction of baryonic mass into stars in times much shorter than a gigayear.

Observations in the Milky Way and other star-forming regions in nearby external galaxies indicate that star formation most easily takes place in overpressured regions where the increased pressure reduces the value of the Jeans mass M_J ($M_J \propto P^{-1/2}$) and causes masses greater than M_J to become gravitationally unstable and form stars. Such a process of inducing star formation in regions of high pressure was used to explain successfully the alignment effect seen in high-redshift radio galaxies, where it was found that the optical continuum and line emission were aligned with the radio lobe axes (McCarthy et al. 1987; Chambers, Miley, & van Breugel 1987). This is in marked contrast to the low-redshift radio galaxies, where the optical and radio axes are roughly orthogonal to each other. This theory found particular favor with the observation of stellar spectral features by Chambers & McCarthy (1990) in their coadded optical spectra of several aligned high- z radio galaxies. Such an alignment was also observed at the longer infrared wavelengths (Eisenhardt & Chokshi 1990) but the amplitude of alignment was reduced, raising a debate on the nature of underlying and presumably dominant star population within the system. Models by Rees (1989b), Begelman & Cioffi (1989), Daly (1990), and de Young (1989) addressed the various ways by which jets triggered aligned star formation activity. See, however, Daly (1992) for a summary of different models that explain the alignment effect. In partic-

ular, recent observations of extended and large polarization fractions have revived interest in the alternative model of scattering anisotropic nuclear radiation by electrons and/or distributed dust (e.g., Dey et al. 1996; Jannuzi et al. 1995). However, Dey et al. estimate that from 89% to more than 58% of the observed emission comes from a diluting, non-polarized component, and that for dust scattering the expected polarization fraction is very small in the K band, leaving open the possibility of the unpolarized component being stellar in origin.

The present paper further explores the premise of jet-triggered star-forming activity, now in gaseous protogalactic units *before* the primary and large-scale episodes of star formation. In particular, could the higher redshift jets activate star formation in the entire prestellar galaxy-sized units? Could this phenomenon explain the formation of elliptical galaxies by converting dissipative gas in protogalactic units into dissipationless stars on timescales that are short compared to dynamical times within the systems? The observed epoch of primary AGN activity at $z \sim 2-3$ will then also correspond to the principal epoch of galaxy formation in the early history of the universe.

In § 2 we address these issues within the framework of the BC89 model for jet-induced activity within overpressured cocoons around AGNs. This model has been verified numerically by Cioffi & Blondin (1992). Section 3 discusses the source properties that are thus activated by jet-induced effects. Section 4 discusses several implications of such an AGN-rooted origin of elliptical and spheroidal components of disks in explaining several of the observed phenomena, and offers a few predictions of the model for future observations, while § 5 summarizes the main results.

2. GALAXY FORMATION MODEL

The basis for our scenario of the making of the early generation of galaxies is that jets associated with the AGN phenomenon get triggered in gravitationally bound gaseous protogalactic environments via some standard mechanism

of efficient accretion onto central massive black holes. Issues related to forming massive black holes in the centers of protogalaxies at an early epoch under consideration here are specifically avoided (see, however, Turner 1991; Loeb 1993; Haehnelt & Rees 1993; Chokshi, Gorti, & Bhat 1997). This jet activity leads to the formation of overpressured cocoons within which the jets propagate. For a two-phase protogalactic environment (Fall & Rees 1985) with cool clouds at $T \sim 10^4$ K in pressure balance with hot ambient gas at $T_a \sim 10^6$ K, the further overpressuring within the radio cocoon results in a sudden reduction of Jeans mass and triggers a synchronized burst of star formation over the cocoon volume (Rees 1989b; BC89). The formation of stars makes this clumped-baryonic content of protogalaxies dissipationless, thereby preserving the ellipsoidal-to-spherical morphology of cocoons—depending on the jet luminosity. We use the simple analytical treatment for overpressured radio cocoons as presented by BC89 with an additional time-varying cross section for the jet head that results from the numerical treatise on radio-jet propagation by Cioffi & Blondin (1992).

Below, we briefly outline a few of the salient points of the BC89 model for overpressured cocoons. In simplest terms, the model construction is based on two equations. The first is an equation for the thrust balance of supersonic jets against the ram pressure of the intergalactic medium (IGM),

$$\rho_a V_h^2 A_h = L_j / v_j, \quad (1)$$

where v_h is the velocity at which the heads of the jets ram into the surrounding medium, L_j is the jet luminosity, ρ_a is the density of the ambient medium into which the jets propagate, v_j is the jet speed, and A_h is the cross-sectional area of the shocked region at the jet head. Using the notation in BC89, the length of the cocoon is given by

$$l \sim v_h t \sim \sqrt{\frac{L_j}{\rho_a v_j A_h}} t. \quad (2)$$

The second is the equation of the static pressure that builds up with time within the cocoon and drives its sideways expansion:

$$\rho_a v_c^2 A_c = L_j / v_h. \quad (3)$$

The width of the overpressured cocoon region is derived from the mean cross-sectional area of the cocoon $A_c \sim v_c^2 t^2$, where v_c is the sideways expansion velocity of the cocoon due to its internal pressure. The width w is then given by

$$w \sim v_c t \sim \left(\frac{L_j v_j A_h}{\rho_a} \right)^{1/8} t^{1/2}. \quad (4)$$

If the static pressure that builds up within the cocoon exceeds the ram pressure of the jets at the head, the cocoon evolution follows the adiabatic spherical expansion of a stellar bubble and is given by

$$R \sim (L_j / \rho_a)^{1/5} t^{3/5}. \quad (5)$$

The cocoon around the AGN remains overpressured as long as its expansion velocity v_c is greater than the sound speed in the medium. For a virialized protogalaxy to be overpressured, the expansion velocity must exceed its velocity dispersion, which is typically ~ 200 km s⁻¹. For the purposes of the present treatment, the main departure from the conventional application of the jet-driven cocoon

model, to Cygnus A and to radio galaxies at moderate redshifts ($z = 1-2$), comes from using ρ_a to be the ambient gas density within the protogalactic environment rather than that of the IGM. In our definition of the term, a “protogalaxy” (PG) refers to a two-phase, gaseous, gravitationally self-supporting system before the primary episode of large-scale star formation. The two components correspond to the hot-phase component virialized with the gravitational potential and in pressure balance with cool photoionized clumps at $T \sim 10^4$ K. For $M_{\text{baryon}} = 10^{11} M_\odot$, and $R \simeq 10$ kpc, the corresponding density $\simeq 0.15$ cm⁻², which implies densities of ~ 15 cm⁻³ at 1 kpc assuming the isothermal density profile. While these numbers reflect average densities within the radii in consideration, stellar-core densities in galaxies approach remarkably high values of $10^5 M_\odot$ pc³ and upward (Lauer et al. 1992; Eckhart et al. 1993), while nuclear gas densities for local examples of starbursting galaxies can also approach similar numbers within $a \sim 1$ kpc radius (Sanders 1992; Scoville 1992) with the dynamical mass within these regions closely approaching the observed stellar and gas mass with a large filling factor.

In the absence of detailed structural information on the density distribution within protogalactic systems, we examine the simplest case of constant-density protogalaxies. Such a model finds some support in a recent study by Mo & Miralda-Escudé (1996) of the gas-phase component of a model protogalaxy to explain the QSO absorption-line systems. Their model requires large-core radii (≤ 100 kpc for $z = 2-3$) with a flat density distribution of the hot gas component for typical M_* -type systems. Outside the core, the gas component follows the (dark) matter distribution with an r^{-2} profile. Cooler component clumps separate out of this hot, gaseous component at sites of pre-existing inhomogeneities or arise from interstellar gas ram-pressured off a satellite galaxy and accreting onto the system and are in pressure equilibrium with this hot component. In the model for jet propagation, the ambient density against which the jets propagate corresponds to that of the hot component, while the associated star formation occurs in a clump component that is left behind in an overpressured environment.

In the present model, we consider protogalaxies of constant densities ranging from that of dense molecular cloud complexes with $n_a \simeq 10^4$ cm⁻³ to the more diffuse ISM densities of a few per cm³ within which the jets propagate. The real situation is bound to be more complex with high gas densities and high cloud-filling factors in protogalactic nuclei to lower ambient densities and far lower filling factors at the effective radii of the protogalactic systems.

An uncertain parameter in the above equations is the value for A_h , which depends on the time-average of jet fluctuation and the corresponding area it influences. We choose a value of $A_h = 30$ kpc² to roughly match the observations of Cyg A. Further, the jet-head area is assumed to vary as the square root of time as for the lightest jets in Cioffi & Blondin’s (1992) model. We feel that this is appropriate for the dense gaseous environments in which the earliest jets propagate and should correspond to the smallest jet-to-ambient density ratio in their model. The area of the jet head is normalized to the value at an age of 10^8 yr. The jet speed is assumed to be $v_j = c$, the speed of light, and a moderate jet power of 10^{45} ergs s⁻¹ is adopted.

Figure 1 illustrates the behavior of cocoon velocity, and size as a function of time, for $n_a = 1-10^4$ cm⁻³. Two facts

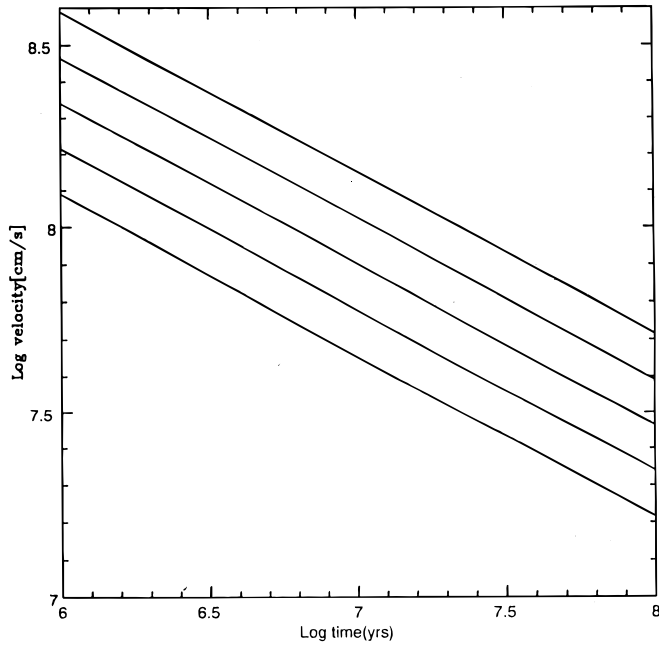


FIG. 1a

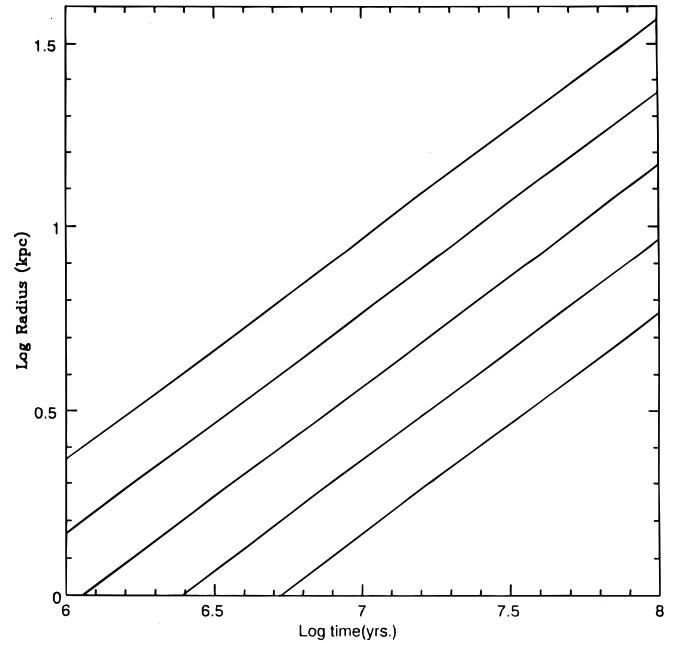


FIG. 1b

FIG. 1.—(a) Velocity evolution of a cocoon driven by a jet of 10^{45} ergs s^{-1} , jet velocity = c , and $A_h = 30$ kpc 2 . The different lines correspond to different adopted ambient densities of $n_H = 1, 10, 10^2, 10^3, 10^4$ cm $^{-3}$, respectively (from top). (b) Radial-size evolution for the same parameters as in (a).

become immediately apparent. First, in all cases for $t \leq 10^8$ yr, the velocity of cocoon expansion exceeds the sound speed in the ambient protogalactic environment, so the cocoon remains overpressured over the lifetime of jet activity, $\leq 10^8$ yr. Second, the cocoon sizes are comparable to the size scales of giant ellipticals for moderate to luminous jet powers and source ages of $\sim 10^7$ – 10^8 yr. If we then use the cocoon model in the context in which it originated and say that these are also the regions over which star formation gets triggered due to overpressuring, then the BC89 model implies that a moderate jet power of 10^{45} ergs s^{-1} is capable of exciting star formation over regions comparable to size scales of present-day galaxies. Note that for the parameters considered here, the static pressure built up over the jet's lifetime is large enough that the cocoon is in a spherical adiabatic expansion mode for homogeneous protogalaxies. This will be discussed further in § 3.2.

3. PROPERTIES OF JET-ACTIVATED PROTOGALAXIES

3.1. Source Sizes

Early work by Rees & Ostriker (1977) showed that large density fluctuations on mass-scales of galaxies $10^{10} M_\odot < M_{\text{gal}} < 10^{12} M_\odot$ were unstable to cooling in H and He recombination and line emission and could not be pressure supported. These fluctuations would undergo isothermal free fall at $\approx 10^4$ K and are capable of fragmentation and subsequent star formation. While the condition of cooling enables fragmentation and subsequent star formation, the latter is not a necessary outcome of an efficient cooling process. Fall & Rees (1985) showed that a collapsing protogalaxy would develop a two-phase structure with the largest cooled units on mass scales of $10^6 M_\odot$ and $T \approx 10^4$ K embedded in hotter ambient galactic medium at its virial temperature of several times 10^6 K. This is the environment where we propose the first AGN-related jet activity to origi-

inate. The relevant masses and radii are $10^{10} M_\odot < M_{\text{gal}} < 10^{12} M_\odot$ and $R \leq 75$ kpc. The discussion in § 2 illustrates that, over a lifetime of jet activity of $\sim 10^8$ yr, it is possible to induce star formation over regions as large as present-day galaxies. Figure 2 shows the effect of varying the jet luminosity on the cocoon parameters. Two jet powers of 10^{43} and 10^{47} ergs s^{-1} are considered to correspond to low-luminosity AGNs and the most powerful systems, respectively. It is seen that the least energetic jets can generate cocoons of size scales relevant to present-day bulges, while the largest size scales available to protogalaxies are easily enveloped in overpressured cocoons on timescales of $\leq 10^8$ yr.

3.2. Source Shapes

Within the framework of the cocoon model, it is found that, except for the most energetic jets, the static pressure vastly exceeds the ram pressure at the jet head, giving rise to adiabatic spherical expansion. Note that the length/width ratio is proportional to $\sim (L_j t)^{1/2}$. Thus for jets of high luminosities and/or long jet durations, the $l > w$ geometries result. This is also true for jets propagating into IGM-type densities encountered for the local examples of radio jets and $z = 1$ – 2 (high- z) radio galaxies displaying the alignment effect (BC89). For the densities considered in this paper, the lower power sources are dominated by static pressure within their cocoons and are in spherical expansion modes through most of their history.

In this context, it is interesting that the observations of galaxy bulges and ellipticals also indicate that the average ellipticity of ellipticals is higher than that corresponding to bulges, as would be expected in the above scenario. Furthermore, the cocoon mechanism naturally explains the formation of disks from low-powered activity in a large galactic size mass fluctuation, which causes stars to form on bulge scales, leaving the remnant baryonic material to settle

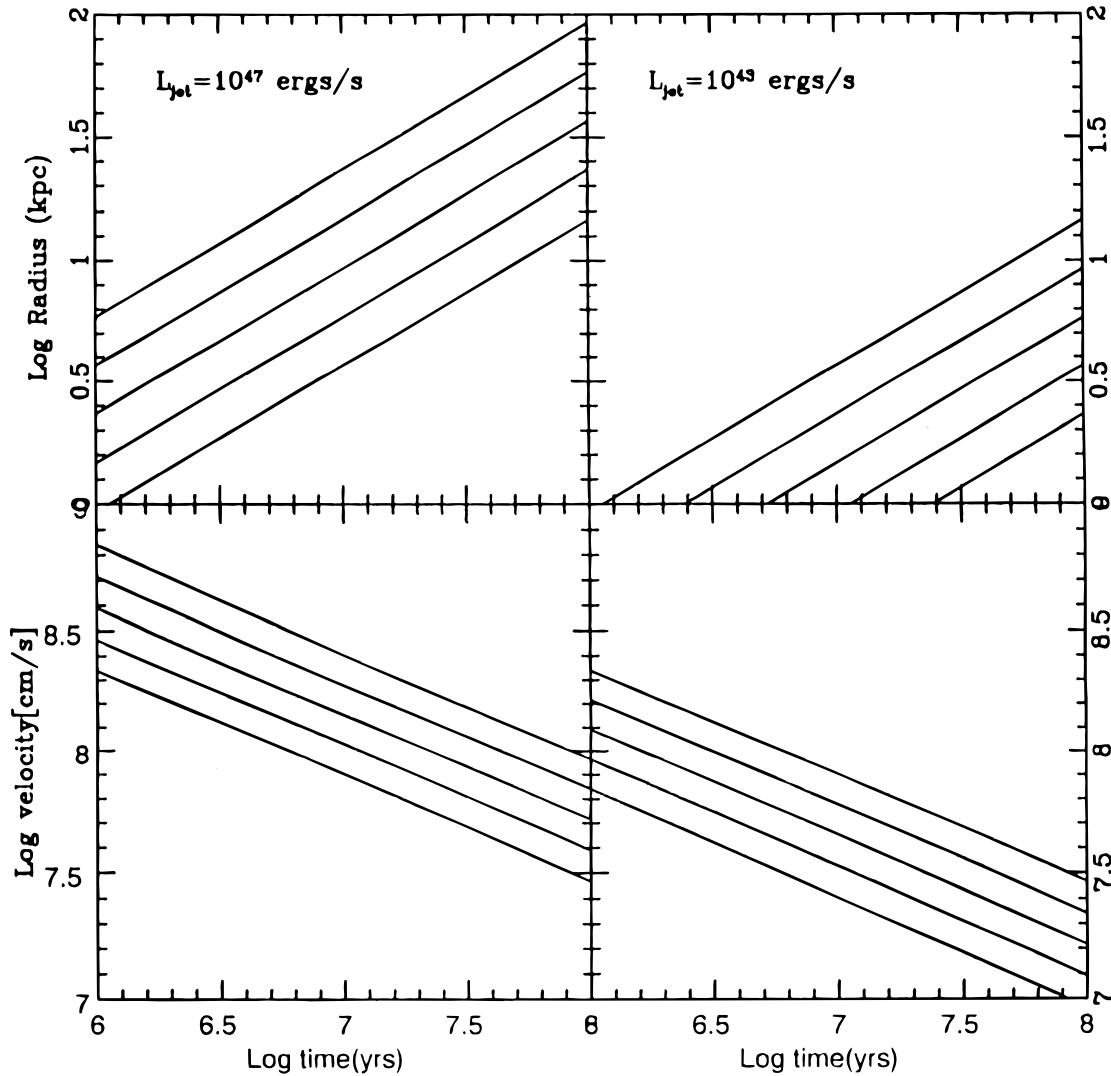


FIG. 2.—Evolution of velocity and size for $L_j = 10^{43}$ and 10^{47} ergs s^{-1}

slowly, conserving angular momentum to a more recent disk morphology. Thus, it would be required that the power of the central engine, and consequently the mass of the massive black hole, scale directly to the spheroidal component of the system rather than to the total mass of the galaxy. This appears to be observationally verified, since the low-power AGNs reside in the centers of Seyfert disks. In particular, kinematic studies of the nuclei of nearby galaxies reveal that the central black hole masses correlate with the bulge luminosities (Kormendy 1994). If one then assumes that central massive black holes, in the presence of a fuel supply, are powered at or near their Eddington luminosity, which is related directly to the observed jet power, then the volume of the cocoon is $\text{Vol.} \sim \frac{1}{2} A_c l$, which, from the previous considerations, gives $\text{Vol.} \propto L_j^{3/4}$. This is the volume converted into stars via the influence of the overpressured cocoon. Assuming a constant M/L ratio and converting to a magnitude scale yields a power-law dependence between black hole (BH) mass (or its Eddington luminosity) and the bulge magnitude with an exponent of $\simeq 1.9$ for the high-luminosity AGNs, while the lower BH masses give rise to spherically expanding cocoons in protogalactic-type environments with volume scales of $\text{Vol.} \propto L_j^{0.6}$, which corresponds to a relation $\log M_{\text{BH}} \propto -1.5 M_{\text{bulge}}$. These two

relations drawn on Figure 3 taken from J. Kormendy (1997, private communication).

3.3. Source Statistics

It is now well established that the population of optically selected, luminous quasars exhibits a peak in number densities between redshifts of $z \simeq 2-3$ (for example, look at the data compilation in Hartwick & Schade 1990). It is further appreciated that the duration of this peak is small compared to the age of the universe (Rees 1990), raising questions about its synchronization over the whole sky and the origin of this epoch of AGN activity in the early universe. While early works focused only on the most luminous QSOs ($M_B < -26$), it is now realized that this enhancement of QSO activity is observed over a range of 5 in absolute magnitude (see Fig. 2 of Hartwick & Schade 1990), corresponding to a factor of 10^2 in intrinsic flux levels. Thus the early results for the most luminous QSOs appear to be sampling the tip of the iceberg, with the less luminous populations following suit.

At the same time, the homogeneity in the photometric properties of spheroids argues for an old stellar content and is consistent with a common epoch for their origin in the early history of the universe. If it is hypothesized that the

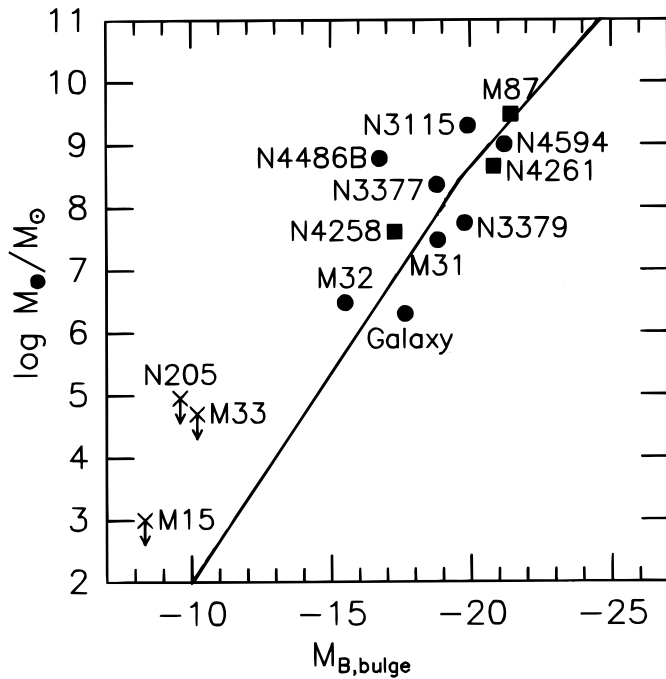


FIG. 3.—Data of Kormendy (1995) with the fits expected from the cocoon-driven model, using arbitrary normalization.

formation of early-type galaxies and bulges is closely linked with the observed optical quasar/AGN peak or epoch, then it is necessary that the number of AGNs at their peak activity (with $z \sim 2-3$) makes up a substantial fraction of the spheroidal population that we see today.

The characteristic QSO density at $z \sim 0$ from the Boyle et al. (1991) sample is

$$\phi_0(z \sim 0) = 5.6 \times 10^{-6} h^3 \text{ Mpc}^{-3} \quad (6)$$

at $M_B = -20.9 + 5 \log h$ for $q_0 = \frac{1}{2}$. Folding in the evolutionary factor of ~ 300 seen in the increase of the brightest QSO number densities yields

$$\phi_0(z \sim \text{peak}) = 0.0017 h^3 \text{ Mpc}^{-3}, \quad (7)$$

which is consistent with the characteristic number density of the entire local galaxy population. Thus, the peak QSO activity certainly has enough numbers to accommodate the observed numbers of normal galaxies in the local universe.

It may be argued that the observed *optical* quasar phenomenon is not associated with jet activity that leads to the production of overpressured cocoons within which the jets propagate. Thus, a model of jet-induced star formation cannot be used to make “visible” galaxies from an optical quasar population. If one uses only the observed radio population, then the present number densities of radio galaxies integrated a decade below their characteristic luminosity at the knee of the luminosity function is $10^{-6} h^3 \text{ Mpc}^{-3}$ (Peacock 1995). Further, an evolutionary model which explains the radio-source counts has the steep-spectrum bright radio sources increase their numbers by a factor of $\sim 10^2$ at a peak active period that roughly matches the epoch when the numbers of optical quasars peak (see Fig. 5 of Dunlop & Peacock 1990). Thus, at peak activity levels, these numbers fall short of the total number densities

of galaxies by roughly a factor of 10. It is well known that the powerful radio galaxies preferentially reside in giant ellipticals, which make up roughly a tenth of the local population of normal galaxies. Thus, to an order of magnitude, it appears that at peak radio activity, there are sufficient numbers of powerful radio galaxies to account for the elliptical galaxy population today. This is fully consistent with the radio observations of optically complete samples by Sadler et al. (1989), which detect that 70% of ellipticals show evidence of nuclear nonthermal emission.

It is, however, useful to note at this stage that two independent models exist that attempt to unify the radio activity in an AGN with an overall evolutionary scheme. For example, Blandford (1994) contends that in the radio-quiet AGNs, the hydromagnetic jets get snuffed out as a result of loading by stellar winds, SNRs, etc. Thus, AGNs begin with radio activity as an integral part of their active phase, create overpressured regions, and ignite star formation, which subsequently extinguishes the radio activity. In the model by Rawlings (1994), radio-quiet sources evolve to radio-loud AGNs when the accretion rate falls below the Eddington limit. Either of these scenarios suggests a duration of radio activity that is less than or equal to the total active phase within the systems. Considerations of sizes of powerful radio doubles, estimates from spectral aging, and ram pressures at the heads of radio sources yield ages of $\sim 10^7$ yr for radio sources. On the other hand, if optical activity in QSOs is driven by accretion processes at roughly the Eddington rate, then the implied duration of activity is roughly a few times 10^7-10^8 yr, assuming the observations of QSOs correspond to several short-duration active phases and lead to remnants of $\sim 10^7 M_\odot$ within most present-day galaxies (Rees 1986). Independent arguments based on observations by Soltan (1982) and Chokshi & Turner (1992) lead to similar estimates for masses of dead quasars in present-day galaxies. Such considerations of ages also match the observed statistics of radio-bright versus quiet quasars; roughly 10% of optical quasar samples are radio-bright, and this ratio does not appear to evolve with redshift to a highest redshift of ~ 3 (Hooper et al. 1996). Thus, duty-cycle considerations also imply that the radio-bright population is undersampled by roughly a factor of 10, corresponding to the ratio of the radio to the optical life cycles, and factoring this into the radio-source counts can provide a sufficiently large population at peak activity to correspond to all spheroidals seen today.

3.4. Source Location

In this paper we specifically avoid a quantitative treatise on the issue of seed BH formation in the centers of galaxies. Given that these small-scale, large $\delta\rho/\rho$ fluctuations arise on galactic-scale perturbations, which in turn lie on a more general large, cluster-scale, milder density perturbation, $\delta\rho/\rho \sim 1$, then the fluctuations are able to grow more efficiently in environs of positive $\delta\rho/\rho$ with material available to accrete than in lower density environs. That is, the absolute depth of a gravitational potential well is deepest when residing on an already existing potential well (see Fig. 9 in Rees 1989a). Thus, one can envisage that the more intense activity associated with larger $\delta\rho/\rho$ in a protocluster environment proliferates preferentially, making elliptical galaxies, while the seed fluctuations in less dense fields will grow via a slow accretion-based process under more difficult, material deficient conditions and lead to bulge forma-

tion of disks in fields. This provides a qualitative explanation for the morphology-density relation, where the morphologically early populations exhibit a marked preference for the richer clusters, while the morphologically late-type systems reside in poorer cluster environments. Then, for a spectrum of fluctuations on a galactic scale, the high incidence of dwarf ellipticals in rich clusters can be understood as arising from bulge formation associated with the less active system and ram-pressure stripping of the gaseous material in rich cluster/dynamically active fields via the process of galaxy harassment (Moore et al. 1996).

3.5. Source Epoch

We have so far illustrated that AGN-driven jet activity is capable of forming spheroids from ~ 1 kpc-scale to ≤ 100 kpc. We have further shown that the observed AGN population at the epoch of peak activity is consistent with accounting for the locally observed spheroid population. However, as previously emphasized in the literature, it is difficult to explain the global synchronization of peak activity over all the sky. The fundamental and global parameter governing structure formation is gravity, and, based on simple considerations of nondissipative gravitational clustering, Rees & Ostriker (1977) showed that clusters of galaxies turned around and separated from the general Hubble expansion at $z \leq 3$. In a more detailed consideration, Bekenstein & Maoz (1989) showed that in Friedmann $\Omega_0 < 1$ models, only for the lowest density models do the richest clusters turn around at $z \simeq 3$, while in dense-universe models the turnaround happens at $z \leq 2$. This also roughly equals the observed epoch of peak QSO activity. If one then demands a causal connection between the cluster turnaround on large scales and AGN activity in galactic nuclei, one is led to a scenario where the nascent BHs in centers of galaxies that were primarily increasing mass via accretion processes from parent galaxies that participated in the general Hubble expansion suddenly find themselves in the dynamically active environments of their host cluster system. Tidal interactions and mergers are able to feed the central black holes, leading to enhanced AGN activity that is synchronized all over the sky. Further, this explains the narrowness of the optical QSO peak of $\Delta t \sim 10^8$ yr as arising from the dynamical/merger-driven activity of similar duration for interactions between normal galaxies. Such suggestions of an interaction-driven active phase can be found in the literature (e.g., Sholsman 1994; Stockton 1990; Heckman 1989; Hutchings & Neff 1992). In the present context, it provides a mechanism for explaining the peak in the AGN and, therefore, the galaxy formation phase via merger activity in cluster potentials separating out of the general Hubble expansion.

4. DISCUSSION

4.1. *K*-Hubble diagram

The existence of the so-called *K*-Hubble diagram for the first-rank ellipticals in rich clusters at low z to the powerful radio galaxies at the highest z has been viewed as a problem for scenarios of induced star formation activity in the early universe at $z \sim 2$. The *K*- z tightness reflects the sampling of an infrared “standard candle” and presumably also of constant mass (for a constant M/L) raising the puzzle of how powerful radio galaxies at high z which display the alignment effect in the optical and the infrared can also behave as

standard candles in the *K* band (Lilly 1990; Chokshi & Eisenhardt 1991).

Within the present scenario, large-scale star formation in all galaxies proceeds via a jet-driven activity at the epoch of peak AGN activity. The most powerful jets were able to affect the entire dynamically distinct gaseous system and convert it into stars, whereas lower level activity could trigger star formation over much smaller volumes and made smaller ellipticals and bulges of galaxies. Given that there is an upper mass cutoff to galactic mass scales dictated by simple considerations of cooling versus dynamical time-scales (Rees & Ostriker 1977), the most powerful radio jets are then able to trigger star formation over this entire protogalactic unit, thus creating the necessary standard candle. One expects that the tightness of the *K*- z relation will be diminished when systems of lower radio luminosity are included. In the lower powered Parkes Selected Regions sample of Dunlop & Peacock (1989), there indeed appears to be such a marginal trend to deviate from the tight *K*-band Hubble sequence. These low-powered systems also do not exhibit the marked alignment between their radio and optical axes (Dunlop & Peacock 1993), as expected because of their lower powers from the cocoon model. Nath (1995) explicitly derives the dependence between the source length and the radio power $l \propto P_{\text{radio}}^{0.3}$ for the BC89 model, which has some observational support in Oort et al. (1987).

4.2. Hosts of AGNs

McLeod & Rieke (1994, 1995) have carried out ground-based near infrared observations of QSO hosts and find that the host isophotes of their low-luminosity sample were consistent with exponential profiles, had bluer $V-H$ colors and resided in typical L^* galaxies, while the more luminous QSO samples resided preferentially in more luminous (and probably also more massive) hosts while their $V-H$ colors were compatible with elliptical hosts. These observations are in complete agreement with expectations from the present model (see § 3.2).

Recent *HST* observations of quasar hosts by Disney et al. (1995); and Bahcall et al. (1995a, 1995b, 1996) found that irrespective of radio loudness, the quasar hosts appeared to be elliptical galaxies with a high incidence of close companions, suggesting tidal interaction and black hole fueling. In particular, observations of PKS 2349–014 show thin wisps, large off-center nebulosity, and the presence of close (< 3 kpc) companions, suggestive of strong tidal interaction (Bahcall et al. 1995b). In the case of an observed spiral quasar host (Bahcall et al. 1996), the system shows a large bulge/disk ratio, implying, within the current framework, the origin of its spheroidal component in luminous jet-driven activity from a massive central black hole.

In our scenario, the most luminous AGNs made the biggest spheroids during their first radio-luminous phase. Further, current reactivation in either the radio or the optical requires fueling of the latent quasar. This is the general spirit of the “feast or famine” model by Blandford (1986), developed further by Small & Blandford (1992). Thus, there appear to be two contending factors that determine the activity level from the central engine. First is the accretion rate—and given sufficient accretion the black hole mass appears to play a role in limiting the total emission at the Eddington rate or less. Thus, one expects the most massive black holes to be capable of most activity, given sufficient accretion. However, the latter is certainly not a

necessary criterion; high-mass black holes can display low activity levels for sufficiently small accretions.

4.3. Quasar Clustering

Smith, Boyle, & Maddox (1995) carried out a cross-correlation study of $z < 0.3$ QSOs and normal galaxies and found that their results were as consistent with similarity in clustering properties of QSOs with galaxies as for galaxy-galaxy clustering. The above result is a natural consequence of the scenario where the QSOs and associated jet-driven activity are responsible for the formation of galaxies.

4.4. Protogalaxies and Protoclusters

Over the last several years, several high-redshift galaxies have been observed that simultaneously show signatures of AGNs and starbursts. Further, it appears that such activity is synchronized in a large number of systems (Steidel et al. 1996) and within clusters (Pascarelle et al. 1996) to a level of few times 10^7 yr. Such synchronized and AGN-associated starburst activity is a natural prediction of the above cocoon-induced galaxy formation scenario. Here we discuss a few individual cases in detail and argue support for our model.

4.4.1. 4C 41.7

This high-redshift radio galaxy at $z = 3.8$ is the most distant example of the alignment effect where the optical continuum and line emissions are collinear with the radio axis of the source (Chambers et al. 1990; Miley et al. 1992). Detailed multiband observations and analyses imply jet powers of $\sim 5 \times 10^{46}$ ergs s^{-1} , an age of $\leq 10^8$ yr, and cold-component densities of several hundred to 1000 cm^{-3} (at $T \simeq 10^4$ K). Optical photometry implies a stellar mass of $3.4 \times 10^{11} M_{\odot}$, with star formation rates in excess of $1000 M_{\odot} \text{ yr}^{-1}$. These high numbers indicate that a large fraction of the total galaxy mass is participating in a starburst on such short timescales, and all observations implicate direct participation of radio jets/cocoons in inducing this starburst. 4C 41.7 then appears to be the most direct example of cocoon-activated galaxy formation.

4.4.2. IRAS FSC 10214+047

Detailed surface photometric and spectroscopic studies of the population of ultraluminous *IRAS* galaxies led Sanders et al. (1988) to propose that galaxy interactions and mergers were enabling large quantities of gas to accumulate in the centers of these systems, which in turn fueled the initial stages of quasar activity and also gave rise to the intense starbursts witnessed in these sources. Most of these ultraluminous sources were residents of the local, low- z Universe. The discovery of the *IRAS* source FSC 10214+047 and its identification with an optical counterpart at $z = 2.28$ (Rowan-Robinson et al. 1991) were interpreted in terms of a highly dust-obscured quasar or a superluminous protogalaxy undergoing an intense starburst involving $\sim 10^{12} M_{\odot}$ on timescales of 5×10^7 yr. These observations provided a high-redshift counterpart to intense starburst activity, with presumably the entire mass of the galaxy participating in the burst. While recent *HST* and ground-based observations (Broadhurst & Lehar 1995; Graham & Liu 1995; Eisenhardt et al. 1996) have shown the system to be strongly lensed with amplification factors

between 5 and 100, the estimated intrinsic luminosity still classifies it as an L^* galaxy in the formation stage.

Based on $1''$ near-infrared imaging spectroscopy of this source, Kroker et al. (1996) find evidence for a significant broad-line component along with extended regions of H α emission and conclude that FSC 10214+047 is an example of an active galactic nucleus enveloped in a circumnuclear starburst region.

4.4.3. Star Formation at $z \leq 3.5$

Steidel et al. (1996) report the discovery of a large number of compact (1.5–3 kpc) star forming galaxies at $3 \leq z \leq 3.5$ with star formation rates of $4\text{--}25 h_{50}^{-2} M_{\odot} \text{ yr}^{-1}$ (they assume $q_0 = 0.5$). While the observed *K*-band photometry can be explained by stellar populations of ≥ 1 Gyr, extinction corrections in the UV could imply ages as short as 10 Myr. Steidel et al. dismiss the latter possibility as unlikely, since it would imply a large number of simultaneously starbursting galaxies at the epoch of observations. The present scenario, however, strongly favors the latter interpretation as arising from the cocoon-driven starbursts associated with the rising part of the high-redshift tail of peak quasar activity. In independent observations, Pascarelle et al. (1996) report the observations at $z = 2.4$ of a galaxy cluster with compact star-forming clumps ~ 1 kpc across. Further, three of their four confirmed cluster members show spectroscopic features indicative of weak AGNs. These results are fully consistent with bulge formation via AGN activity.

4.5. Predictions

Galaxy formation via radio cocoon activity predicts the following:

1. Lower powered radio galaxies and quasars should fall off the *K*-Hubble sequence, while the hosts of the most luminous QSOs should continue to obey the observed sequence.
2. The host ellipticities of the higher powered AGNs should be higher than that of the spheroidal component of the lower powered AGNs.
3. Since star formation is triggered by the action of radio jets, it is expected that the radio-loud systems have systematically younger stellar populations and show brighter and bluer colors than the radio-quiet AGNs. This could be tested for hosts of radio-loud versus radio-quiet QSOs of similar optical brightness.
4. In galaxy spectral energy distribution evolution models presented by Chambers & Charlot (1990), the amplitude of the 4000 \AA break evolves rapidly on timescales of 10^8 yr. Since the star formation proceeds from inside-to-out in the cocoon model over similar timescales, one expects to see bluer colors at large galactocentric distances.
5. Due to the larger stellar contribution at longer (than UV) wavelengths, one expects the polarization fraction to diminish at increasing wavelengths. However, such a prediction is also expected from dust scattering of anisotropic radiation by a central source. It is therefore of key importance that experiments be designed to search for stellar absorption features in the aligned components of high- z radio galaxies.

5. SUMMARY

This paper proposes that there are significant advantages to reversing the sequence of the AGN–galaxy formation

association, with AGN activity causing the formation of the primary generation of stars in elliptical and spheroidal components of disks. The simple model of BC89 provides an adequate vehicle to illustrate the feasibility of such a scenario, while the statistics of AGN populations at high z allow such jet-induced galaxy formations in sufficient numbers to account for the entire local galaxy population.

Among the primary advantages of such an AGN-triggered formation mechanism for galaxies are the

resolution of the K -Hubble diagram and an explanation for quasar correlations and properties of distant galaxies that show coexisting signatures of AGNs and starbursts.

I gratefully acknowledge useful discussions with Harish Bhat, Peter Eisenhardt, Biman Nath, and Kandu Subhramaniam. I thank the anonymous referee for making me think some more. I thank J. Kormendy for providing Figure 3 presented in this paper.

REFERENCES

- Bahcall, J. N., Kirhakos, S., & Schneider, D. P. 1995a, *ApJ*, 450, 486
 ———. 1995b, *ApJ*, 447, L1
 ———. 1996, *ApJ*, 457, 486
 Begelman, M. C., & Cioffi, D. F. 1989, *ApJ*, 345, L21
 Bekenstein, J. D., & Maoz, E. 1989, in *The Epoch of Galaxy Formation*, ed. C. S. Frenk (Dordrecht: Kluwer)
 Blandford, R. 1986, in *IAU Symp. 119, Quasars*, ed. G. Swarup & V. Kapahi (Dordrecht: Reidel), 359
 Blandford, R. 1994 in *ASP Conf. Proc. 54, The First Stromlo Conference: The Physics of Active Galaxies*, ed. G. V. Bicknell, M. A. Dopita, & P. J. Quinn (San Francisco: ASP), 23
 Boyle, et al. 1991, in *ASP Conf. Ser. 21, The Space Distribution of Quasars*, ed. D. Crampton (San Francisco: ASP)
 Broadhurst, T., & Lehar, J. 1995, *ApJ*, 450, L41
 Chambers, K. C., & Charlot, S. 1990, *ApJ*, 348, L1
 Chambers, K. C., & McCarthy, P. J. 1990, *ApJ*, 354, L9
 Chambers, K. C., Miley, G. K., & van Breugel, W. 1987, *Nature*, 329, 604
 ———. 1990, *ApJ*, 363, 21
 Chokshi, A., & Eisenhardt, P. R. M. 1991, *Comments Astrophys.*, 15, 343
 Chokshi, A., & Turner, E. L. 1992, *MNRAS*, 259, 421
 Chokshi, A., Gorti, U., & Bhat, H. 1997, in preparation
 Cioffi, D. F., & Blondin, J. M. 1992, *ApJ*, 392, 458
 Daly, R. 1990, *ApJ*, 355, 416
 ———. 1992, in *First Light in the Universe*, ed. B. Rocca-Volmerange et al., (Gif-sur-Yvette: Editions Frontières), 131
 de Young, D. 1989, *ApJ*, 342, L59
 Dey, A., et al. 1996, *ApJ*, 465, 157
 Disney, M. J., et al. 1995, *Nature*, 376, 150
 Dunlop, J. S., & Peacock, J. A. 1989, *MNRAS*, 238, 1171
 ———. 1990, *MNRAS*, 247, 19
 ———. 1993, *MNRAS*, 263, 936
 Eckart, A., Genzel, R., Hoffman, R., Sams, B. J., & Tacconi-Garman, L. E. 1993, *ApJ*, 407, L77
 Eisenhardt, P. R. M., & Chokshi, A. 1990, *ApJ*, 351, L9
 Eisenhardt, P. R. M., Armus, L., Hogg, D. W., Soifer, B. T., Neugebauer, G., & Werner, M. W. 1996, *ApJ*, 461, 72
 Fall, M. S., & Rees, M. J. 1985, *ApJ*, 298, 18
 Graham, J. R., & Liu, M. 1995, *ApJ*, 449, L29
 Haehnelt, M. G., & Rees, M. J. 1993, *MNRAS*, 263, 168
 Hartwick, F. D. A., & Schade, D. 1990, *ARA&A*, 28, 437
 Heckman, T. M. 1989, in *IAU Colloq. 124, Paired and Interacting Galaxies*, ed. J. Sulentic & W. Keel (Washington DC: NASA), 359
 Hooper, P. C., et al. 1996, preprint
 Hutchings, J. B., & Neff, S. G. 1992, *AJ*, 104, 1
 Januzzi, B. T., et al. 1995, *ApJ*, 454, L111
 Kormendy, J. 1994, in *Nuclei of Normal Galaxies*, ed. R. Genzel & A. I. Harris (Dordrecht: Kluwer), 379
 Kroker, H., Genzel, R., Krabbe, A., Tacconi-Garman, L. E., Tecza, M., Thatte, N., Beckwith, S. V. W. 1996, *AJ*, 463, L55
 Lauer, T. R., et al. 1992, *AJ*, 104, 552
 ———. 1990, in *ASP Conf. Ser. 10, Evolution of the Universe of Galaxies*, ed. R. G. Kron (San Francisco: ASP), 344
 Loeb, A. 1993, *ApJ*, 403, 542
 McCarthy, P. J., Spinrad, H., Djorgovski, S., Strauss, M. A., van Breugel, W. J. M., & Liebert, J. 1987, *ApJ*, 319, L39
 McLeod, K., & Rieke, G. 1994, *ApJ*, 420, 58
 ———. 1995, *ApJ*, 454, L77
 Miley, G. K., Chambers, K. C., van Breugel, W. J. M., & Macchetto, F. 1992, *ApJ*, 401, L69
 Mo, H. J., & Miralda-Escudé, J. 1996, *ApJ*, 469, 589
 Moore, B., Katz, N., Lake, G., Dressler, A., & Oemler, Jr., A., 1996, *Nature*, 379, 613
 Nath, B. B. 1995, *MNRAS*, 274, 208
 Oort, M. J. A., Katgert, P., & Windhorst, R. A. 1987, *Nature*, 328, 500
 Partridge, R. B., & Peebles, P. J. E. 1967, *ApJ*, 147, 868
 Pascarelle, S. M., et al. 1996, *ApJ*, 456, L96
 Peacock, J. A., 1995, in *StScI Symp. 7, Extragalactic Background Radiation*, ed. D. Calzetti, M. Livio, & P. Madau (Cambridge: Univ. Press), 237
 Rawlings, S. 1994, *ASP Conf. Ser. 54, The First Stromlo Conference: The Physics of Active Galaxies* ed. G. V. Bicknell, M. A. Dopita, & P. J. Quinn (San Francisco: ASP), 253
 Rees, M., 1986, in *IAU Symp. 119, Quasars*, ed. G. Swarup, & V. Kapahi (Dordrecht: Reidel), 1
 ———. 1989a in *Evolutionary Phenomena in Galaxies*, ed. J. E. Beckman, & B. E. J. Pagel (Cambridge: Cambridge Uni. Press), 1
 ———. 1989b, *MNRAS*, 239, 1P
 ———. 1990, *Science*, 247, 817
 Rees, M. J., & Ostriker, J. 1977, *MNRAS*, 179, 541
 Rowan-Robinson, M., et al. 1991, *Nature*, 351, 719
 Sadler, E. M., Jenkins, C. R., & Kotanyi, C. G., 1989, *MNRAS*, 240, 591
 Sanders, D. B., et al. 1988, *ApJ*, 325, 74
 Sanders, D. B. 1992 in *ASP Conf. Ser. 31, Relationships between AGNs and Starburst Galaxies*, ed. A. V. Filippenko (San Francisco: ASP), 303
 Scoville, N. Z., 1992, in *ASP Conf. Ser. 31, Relationships between AGNs and Starburst Galaxies*, ed. A. V. Filippenko (San Francisco: ASP), 159
 Sholsman, I., ed. 1994, *Mass Transfer Induced Activity in Galaxies* (New York: Cambridge Univ. Press)
 Small, T. A., & Blandford, R. D. 1992, *MNRAS*, 259, 725
 Smith, R. J., Boyle, B. J., & Maddox, S. J. 1995, *MNRAS*, 277, 270
 Soltan, A. 1982, *MNRAS*, 200, 115
 Steidel, C. S., Giavalisco, M., Pettini, M., Dickinson, M., & Adelberger, A. 1996, *ApJ*, 462, L17
 Stockton, A. 1990, in *Dynamics and Interactions of Galaxies*, ed. R. Wielen (Berlin: Springer), 440
 Turner, E. L. 1991, *AJ*, 101, 5